J. Electrochem. Sci. Eng. **16** (2026) 3126; https://doi.org/10.5599/jese.3126

Open Access : : ISSN 1847-9286
https://pub.iapchem.org/ojs/index.php/JESE

Original scientific paper

Bismuth molybdate nanostructure modified carbon paste electrode for voltammetric sensing of levodopa in the presence of acetaminophen

Abdul Amir H. Kadhum[1], Ahmed J. Allami[2,3], Hajir M. Ali[4] and Huda Hadi Nameh[5,✉]

[1]*College of Medicine, University of Al-Ameed, Karbala, Iraq*
[2]*Department of Physiology, College of Medicine, University of Kirkuk, Kirkuk 36001, Iraq*
[3]*Cental Technology, Komar University of Science and Technology, Sulaymaniyah, Iraq*
[4]*Department of Biomedical Engineering, Al-Khwarizmi, College of Engineering, University of Baghdad, Baghdad, Iraq*
[5]*College of Pharmacy, University of Hilla, Babylon, Iraq*

Corresponding Author: E-mail: ✉huda_hadi@hilla-unc.edu.iq

Received: November 22, 2025; Accepted: December 6, 2025; Published: May 10, 2026

Abstract

In the present work, a voltammetric sensor for levodopa (L-DOPA) was fabricated based on Bi_2MoO_6 nanostructure-modified carbon paste electrodes (Bi_2MoO_6/CPE). Bi_2MoO_6 nanostructures were synthesized via the solvothermal procedure and characterized by X-ray diffraction pattern. The Bi_2MoO_6/CPE exhibited an enhanced current response for L-DOPA, which we attribute to the good electrocatalytic activity of the Bi_2MoO_6 nanostructures. Furthermore, the Bi_2MoO_6/CPE sensor was applied to determine L-DOPA in the presence of acetaminophen (ACT). The anodic peaks for L-DOPA and ACT were well-resolved in their mixture, enabling their simultaneous determination. The voltammetric measurements at pH 7.0 revealed distinct anodic peaks for the two analytes, located at approximately 350 mV (L-DOPA) and 530 mV (ACT). Using differential pulse voltammetry, a linear correlation was observed between the oxidation peak current and L-DOPA concentration over the range 0.02 to 590.0 μM. The limit of detection was determined to be 0.009 μM. The practical applicability of the Bi_2MoO_6/CPE sensor was successfully demonstrated through the assay of L-DOPA and ACT in real samples.

Keywords

Parkinson's disease; Bi_2MoO_6 nanostructures, real sample analysis, chronoamperometry

Introduction

Parkinson's disease is a widespread condition affecting the nervous system, marked by the gradual, ongoing degeneration of dopamine-producing nerve cells in a specific area of the midbrain

known as the substantia nigra pars compacta. Thus, this progressive neurological condition arises from a significant deficiency in the brain's dopamine production. The incidence of Parkinson's disease increases markedly with age, with the majority of cases emerging in older adulthood. This dopamine deficiency causes several movement-related issues, including tremors, slowed action execution (bradykinesia), muscle stiffness, and an unsteady posture [1-3].

Direct administration of dopamine is ineffective as it cannot cross the blood-brain barrier. For this reason, the precursor molecule levodopa (L-DOPA) is used as a primary treatment in Parkinson's disease, where it is converted to dopamine in the brain [4,5]. As a catecholamine precursor, L-DOPA's primary mechanism of action is enzymatic conversion to dopamine by DOPA decarboxylase. This process effectively counteracts the dopamine deficit characteristic of the disease in the brain. A significant drawback of levodopa therapy is that its conversion to dopamine can also occur in the peripheral tissues, leading to adverse effects, including dyskinesia, gastrointestinal inflammation, paranoid ideation, nausea, and cardiac palpitations. An additional concern is that the metabolism of L-DOPA generates toxic oxidation products, such as semiquinones, quinones, and reactive oxygen species [6-8].

It is also common for individuals with Parkinson's disease to be on long-term regimens that include acetaminophen, opioids, and neuropathic pain medications like certain anticonvulsants and antidepressants [9].

Acetaminophen (ACT), also known as N-acetyl-p-aminophenol or paracetamol, is extensively employed for its pain-relieving and fever-reducing properties. Furthermore, ACT is indicated for symptoms of colds and the flu, including fever and cough, as well as for the relief of mild to moderate pain. These can range from common headaches and toothaches to musculoskeletal discomfort, such as backaches and joint pain. Additionally, individuals suffering from asthma often favor ACT for pain relief. When administered at appropriate therapeutic levels, ACT is readily metabolized by the body. An overdose of ACT results in the buildup of toxic metabolic byproducts, which can induce severe and potentially fatal liver damage, as well as kidney toxicity that may progress to renal failure [10-12].

Since acetaminophen absorption is linked to gastric emptying, other medications that influence gastric motility, including L-DOPA, can affect how the body processes ACT [13,14]. Consequently, the ability to determine the concentrations of L-DOPA and ACT, either simultaneously or individually, is of significant clinical importance.

Electrochemical methods are among the most attractive options for the analysis of pharmaceutical and biological compounds [15,16]. A key strength of electrochemical methods is that they provide analytical solutions distinguished by their instrumental simplicity, low cost, high sensitivity, straightforward miniaturization, portability, and numerous other unique benefits [17-19].

The direct electrochemical analysis of L-DOPA and ACT at unmodified electrodes is hampered by slow electron-transfer kinetics, a consequence of surface fouling caused by the accumulation of their oxidation products. The proximity of the oxidation potentials for L-DOPA and ACT results in significant voltammetric peak overlaps at bare electrode surfaces [20].

The application of conductive materials to modify bare electrode surfaces offers significant benefits for the fabrication of advanced electrochemical sensors. Recently, chemically modified electrodes have been widely employed to separate overlapping voltammetric signals from solution components that overlap at bare electrodes due to closely spaced redox potentials. On the other hand, modified electrodes have been widely adopted as working electrodes in electrochemical sensors due to their broad dynamic range, high sensitivity, low cost, and operational simplicity [21-24].

Carbon paste electrodes (CPEs) are widely used as matrices for modified electrodes because they are easy to prepare, provide a renewable surface, and are compatible with a wide range of modifiers. An additional advantage is their low background current, which is a marked improvement over noble-metal or solid-graphite electrodes [25-28].

Rapid advances in nanotechnology are enabling better ways to build nanostructures, leading to many more applications. The use of electrochemical sensors incorporating diverse nanostructures, including metal oxide nanoparticles, is growing steadily. This trend is driven by their advantageous properties, including superior electrical conductivity, exceptional stability, and rapid electron-transfer rates [29-31].

Nanostructured transition metal oxides are widely regarded as ideal electrode materials for electrochemical sensors, owing to their advantageous characteristics, which include eco-friendliness, straightforward synthesis, low cost, and high abundance [32,33]. In recent years, scientists have investigated transition metal oxides such as MnO_2 [34], Co_3O_4 [35], NiO [36], ZnO [37] and MoO_3 [38] for use in electrode modification. However, the practical deployment of transition metal oxides is hindered by certain limitations, including poor electrical conductivity and low electrochemical stability. The adoption of binary metal oxides (*e.g.* $ZnCo_2O_4$ [39], $NiMoO_4$ [40], $MnMoO_4$ [41]) as alternative electrodes addresses these shortcomings directly. Their capacity for redox reactions, enabled by multiple oxidation states, results in superior electrical conductivity [42]. As a significant member of the metal molybdate family, bismuth molybdate (Bi_2MoO_6) shows considerable potential for use in various fields, including catalysis, energy storage, and gas sensing [43,44]. Recent scientific literature has documented intriguing findings regarding bismuth molybdate-based electrodes for electrochemical sensing [45,46].

This work presents a proposed method for determining L-DOPA using a carbon paste electrode modified with a Bi_2MoO_6 nanostructure (Bi_2MoO_6/CPE). Owing to the good catalytic activity of the Bi_2MoO_6 nanostructure, the fabricated electrode exhibited exceptional analytical performance for the L-DOPA detection. Furthermore, the created electrode was successfully evaluated for the selective voltammetric determination of L-DOPA in the presence of ACT. Finally, the analytical performance of the Bi_2MoO_6/CPE sensor was evaluated for the determination of both L-DOPA and ACT in urine samples.

Experimental

Chemicals and apparatus

All reagents were used as received, without further purification. Experiments were performed using 0.1 M phosphate buffer (PB) solutions at different pH values.

All electrochemical studies were carried out with an Autolab 302N potentiostat/galvanostat (Metrohm, The Netherlands) using GPES software (version 4.9) for data acquisition and control. A three-electrode system consisted of a bare/modified CPE (working electrode), an Ag/AgCl electrode (reference electrode), and a platinum wire (counter electrode). pH measurements and adjustments were performed with a Metrohm 710 pH meter (Switzerland). X-ray diffraction (XRD) patterns were collected on a Panalytical X'Pert Pro diffractometer using Cu-Kα radiation (λ = 0.154 nm).

Synthesis of Bi_2MoO_6 nanostructures

For the synthesis of Bi_2MoO_6 nanostructures, 1 mmol of $Bi(NO_3)_3{\times}5H_2O$ was first dissolved into 10 mL of ethylene glycol containing 1 mmol of $(NH_4)_6Mo_7O_{24}{\times}4H_2O$. Subsequently, 25 mL of ethanol was gradually added to the above solution under continuous magnetic stirring for 30 min. The

resulting mixture was then subjected to ultrasonic treatment for 45 min to ensure proper dispersion of the precursors. Following sonication, the homogeneous solution was transferred to a Teflon-lined autoclave and heated to 160 °C for 12 h in an oven. After the solvothermal reaction, the autoclave was allowed to cool naturally at ambient temperature. The precipitate was collected by centrifugation, thoroughly washed several times with distilled water and ethanol, and finally dried under vacuum at 65 °C overnight to obtain the Bi_2MoO_6 product.

Modification of CPE with Bi_2MoO_6 nanostructures

The Bi_2MoO_6/CPE was prepared by mixing Bi_2MoO_6 and graphite powder in a 4:96 mass ratio. The appropriate amount of paraffin oil was then added and thoroughly blended into the mixture by hand mixing for 60 min. We packed the fabricated paste into a glass tube and established an electrical contact with a copper wire. The surface of the Bi_2MoO_6/CPE was polished with smooth sandpaper before use. For comparison, a bare CPE was prepared using the same method but without Bi_2MoO_6.

Results and discussion

Characterization of Bi_2MoO_6 nanostructures

The crystalline structure of the synthesized Bi_2MoO_6 was examined using XRD pattern, exhibited in Figure 1. The observed diffraction peaks in the recorded XRD pattern are consistent with the crystalline structure of Bi_2MoO_6 [47].

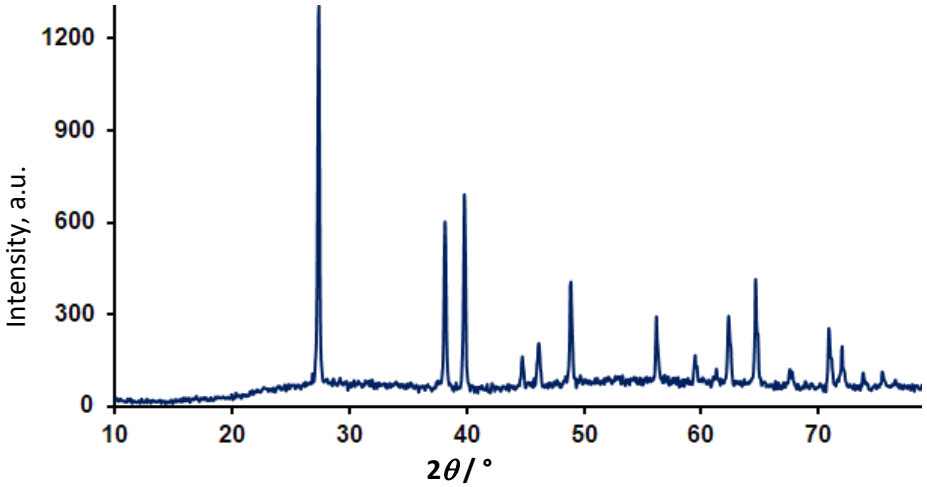

Figure 1. *XRD pattern of Bi_2MoO_6 nanostructures*

Electrochemical behavior of L-DOPA at the Bi_2MoO_6/CPE and bare CPE

The influence of pH on the electrochemical response of L-DOPA at Bi_2MoO_6/CPE was studied in 0.1 M PB over a pH range of 2.0-9.0. The anodic peak current (I_{pa}) increased with pH from 2.0 to 7.0, then decreased at higher pH values (up to 9.0). Consequently, all subsequent experiments were performed in 0.1 M PB as the supporting electrolyte at pH 7.0.

Cyclic voltammetry (CV) was used to compare the electrochemical behavior of the different modified electrodes (Bi_2MoO_6/CPE and bare CPE) toward 300.0 µM L-DOPA (Figure 2). The bare CPE showed only a small anodic peak with I_{pa}=6.07 µA. Modification with Bi_2MoO_6 resulted in a significant increase in the oxidation current. This demonstrates that Bi_2MoO_6 enhances the electrode's conductivity, thereby improving the current response for L-DOPA. As expected, the Bi_2MoO_6/CPE exhibited a superior voltammetric response compared to bare CPE, featuring a higher

peak current and a slightly lower peak potential (I_{pa}=14.5 µA and E_{pa}=350 mV). These results demonstrate the superior electrocatalytic properties of the Bi_2MoO_6 nanostructure for the oxidation of L-DOPA, resulting in signal amplification.

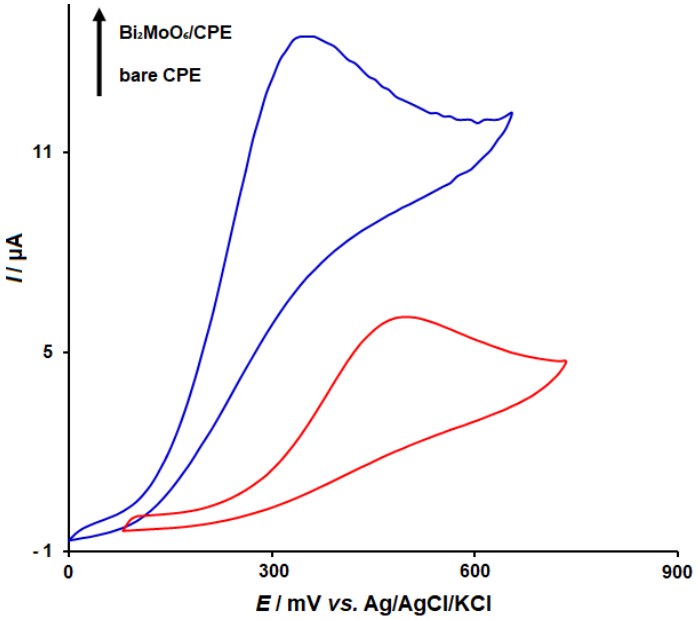

Figure 2. *CV responses of bare CPE, and Bi_2MoO_6/CPE to L-DOPA (300.0 µM) in PB (0.1 M, pH 7.0); scan rate 50 mV s^{-1}*

Influence of scan rate

We studied the influence of scan rate on the L-DOPA oxidation signal at the Bi_2MoO_6/CPE under optimum conditions. Figure 3 displays the cyclic voltammograms of the Bi_2MoO_6/CPE in 100.0 µM of L-DOPA at various scan rates (10 to 250 mV s^{-1}).

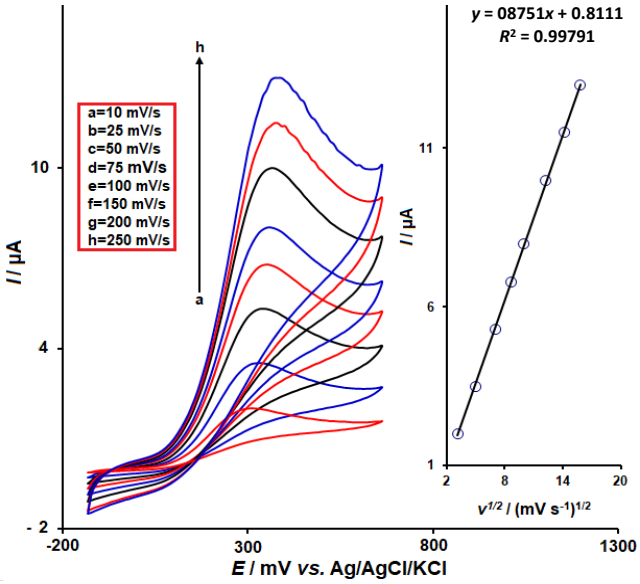

Figure 3. *CV responses of Bi_2MoO_6/CPE to 100.0 µM L-DOPA in PB (0.1 M, pH 7.0) at various scan rates. Inset: Plot of I_{pa} vs. $\nu^{1/2}$*

As the scan rate increased, the anodic current gradually increased, accompanied by a positive shift in the anodic potential. The observed linear dependence of the anodic current on the square root of the scan rate ($\nu^{1/2}$), Figure 3 inset, indicates that the electro-oxidation of L-DOPA is a diffusion-controlled process.

Chronoamperometric studies

The electrocatalytic oxidation of L-DOPA was investigated using chronoamperometry. Figure 4 presents the chronoamperometric responses of the Bi_2MoO_6/CPE at a constant potential of 400 mV. The diffusion coefficient of L-DOPA was determined from these chronoamperograms. We calculated the diffusion coefficient of L-DOPA by applying the Cottrell Equation (1):

$$I_{pa} = nFACD^{1/2}\pi^{-1/2}t^{-1/2} \quad (1)$$

where D / cm² s^{-1} is the diffusion coefficient, and C_b / mol cm^{-3} is the analyte concentration. This investigation utilized L-DOPA at concentrations ranging from 0.3 to 1.5 mM. The chronoamperometric data were analyzed using linear plots of I_{pa} against $t^{-1/2}$ for different concentrations of L-DOPA (Figure 4A). The fitted experimental plots for different L-DOPA concentrations are presented in Figure 4B. Applying the Cottrell equation to the slope of this plot yielded an average diffusion coefficient of 1.2×10^{-6} cm²/s for L-DOPA.

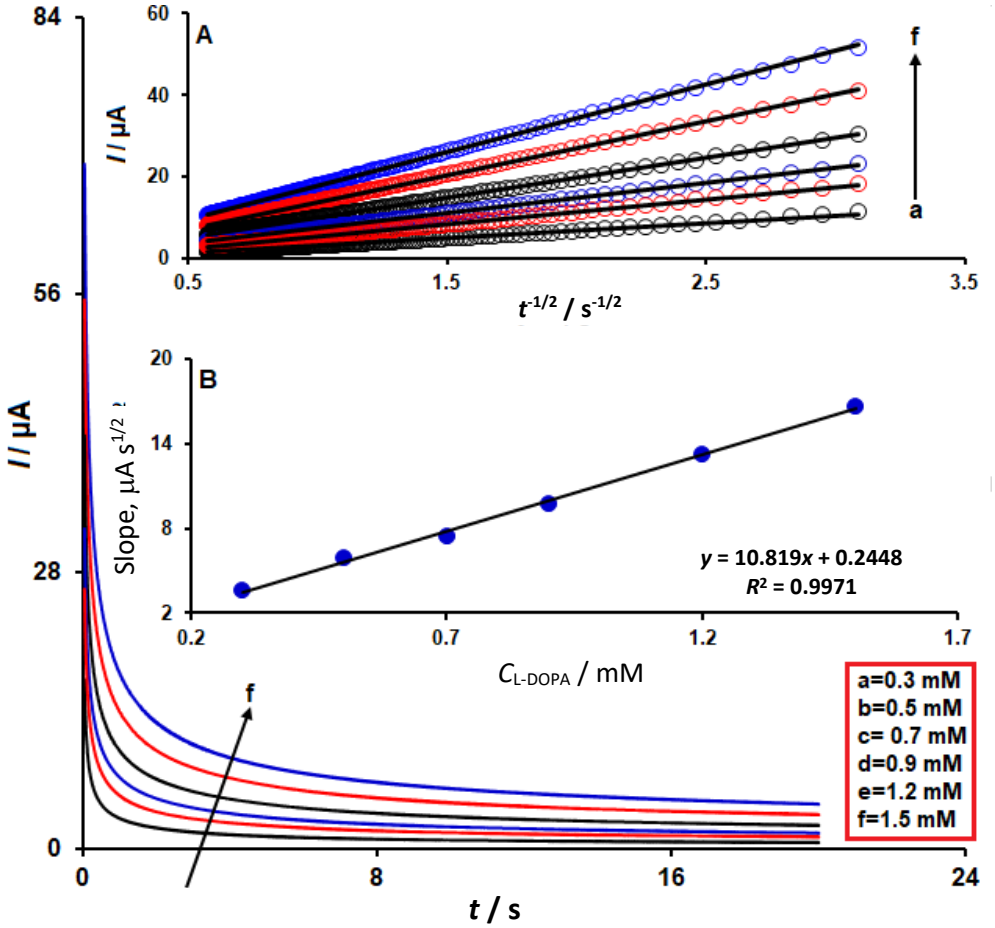

Figure 4. *Chronoamperometric responses of Bi_2MoO_6/CPE to L-DOPA at different concentrations from 0.3 to 1.5 mM in PB (0.1 M, pH 7.0). Linear dependence of I_{pa} on $t^{-1/2}$ (Inset A) and linear dependence of the slope of linear fits on L-DOPA concentration (Inset B)*

Quantitative measurements of L-DOPA at Bi_2MoO_6/CPE sensor using DPV method

Key analytical parameters for L-DOPA determination, including the LOD and linear detection range, were calculated using the highly sensitive DPV method. Figure 5 shows the DPVs obtained for different L-DOPA concentrations at the Bi_2MoO_6/CPE under the optimized parameters. The oxidation peak current increased linearly with the L-DOPA concentration. A linear relationship was observed between the DPV peak current and the concentration of L-DOPA over the range of 0.02 to 590 µM, following the equation: I_{pa}= 0.0462$C_{L\text{-}DOPA}$ + 0.7039 (R^2 = 0.9999). The Bi_2MoO_6/CPE sensor exhibited a LOD of 0.009 µM for L-DOPA.

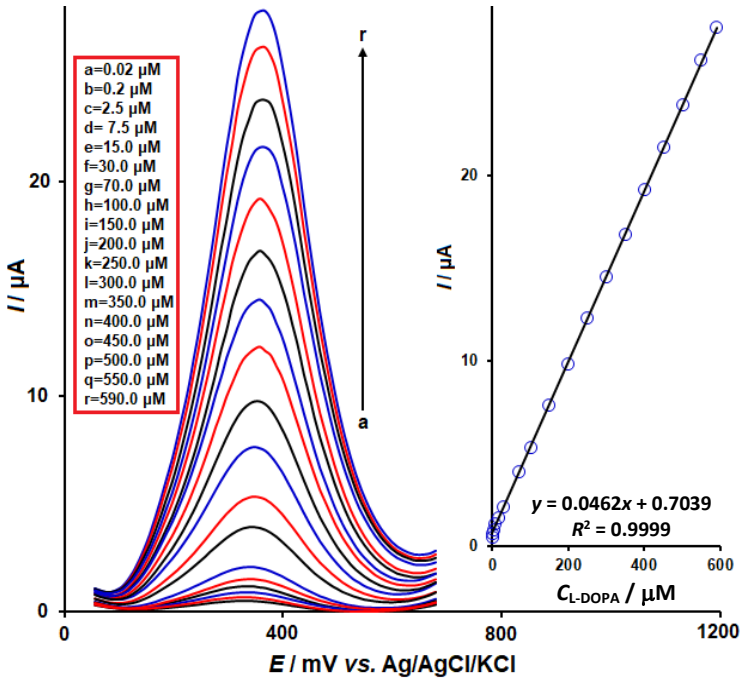

Figure 5. *DPV responses of Bi_2MoO_6/CPE to L-DOPA at different concentrations from 0.02 to 590.0 µM in PB (0.1 M, pH 7.0). Inset: calibration plots of the I_{pa} response vs. L-DOPA concentration*

The simultaneous determination of L-DOPA and ACT at Bi_2MoO_6/CPE sensor

The primary goal of this work was to achieve the simultaneous voltammetric determination of L-DOPA and ACT using a Bi_2MoO_6/CPE. This was accomplished by recording DPVs while simultaneously varying the concentrations of both L-DOPA and ACT. The voltammograms exhibited well-defined anodic peaks for L-DOPA and ACT at 350 and 530 mV, respectively. These results indicate that the simultaneous determination of L-DOPA and ACT is feasible using the Bi_2MoO_6/CPE, as shown in Figure 6.

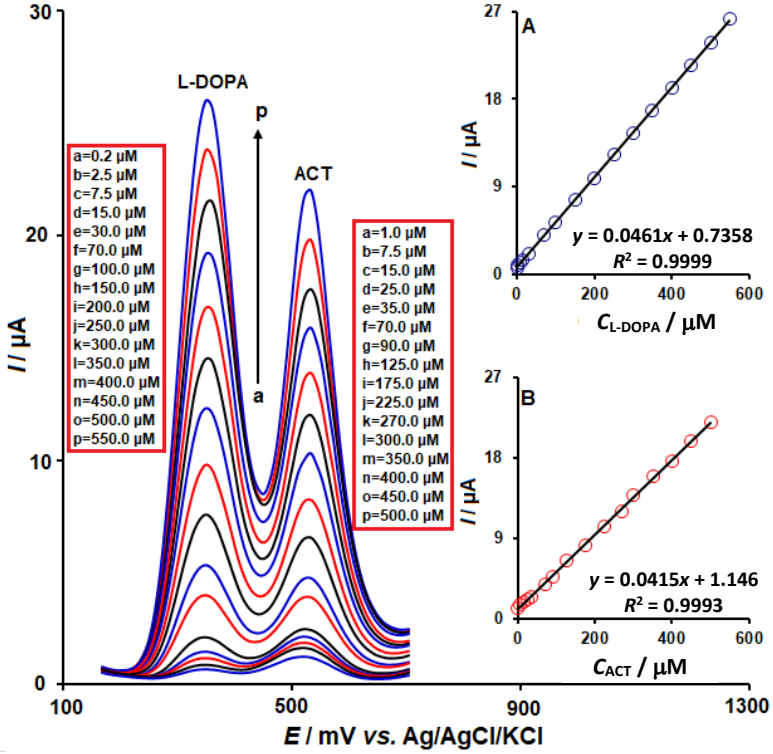

Figure 6. *DPV responses of Bi_2MoO_6/CPE to various concentrations of L-DOPA (from 0.2 to 550.0 µM) and ACT (from 1.0 to 500.0 µM) in PB (0.1 M, pH 7.0). Insets: A) calibration plots of the I_{pa} response vs. L-DOPA concentration and B) calibration plots of the I_{pa} response vs. ACT concentration*

The sensor exhibited a sensitivity of 0.0461 μA μM^{-1} towards L-DOPA in the presence of ACT (Figure 6A). The similar sensitivity in the absence of ACT (0.0462 μA μM^{-1}) indicates that the oxidation processes are independent. This confirms that their simultaneous determination in mixtures is feasible without significant interference.

Application of the Bi_2MoO_6/CPE platform for L-DOPA and ACT analysis in real samples

The practical applicability of the Bi_2MoO_6/CPE was demonstrated by the determination of L-DOPA and ACT in urine samples. Following sample preparation, the L-DOPA and ACT content were quantified by the standard addition method. The corresponding results are compiled in Table 1. As shown in Table 1, the obtained recovery rates of 97.3 to 104.5 % confirm the high accuracy and practical utility of the created electrode for the determination of L-DOPA and ACT in real specimens.

Table 1. *Analysis of real sampled for L-DOPA and ACT determination by Bi_2MoO_6/CPE sensing platform (n = 5)*

Sample	Added concentration, μM		Found concentration, μM		Recovery, %		RSD, %	
	L-DOPA	ACT	L-DOPA	ACT	L-DOPA	ACT	L-DOPA	ACT
Human urine	0	0	-	-	-	-	-	-
	5.0	5.5	4.9	5.6	98.0	101.8	3.0	2.8
	7.0	7.5	7.2	7.3	102.9	97.3	2.2	3.3
	9.0	9.5	8.9	9.8	98.9	103.2	1.9	2.6
	11.0	11.5	11.5	11.4	104.5	99.1	2.7	2.1

Conclusion

In the present study, a L-DOPA sensing electrode was constructed *via* mixing the Bi_2MoO_6 nanostructures, graphite powder. Owing to the catalytic activity of Bi_2MoO_6 nanostructures, the fabricated electrode exhibited exceptional performance in the detection of L-DOPA. The Bi_2MoO_6/CPE exhibited a wide linear detecting range from 0.02 to 590.0 μM and a LOD of 0.009 μM for the detection of L-DOPA. The Bi_2MoO_6/CPE exhibited high selectivity for the simultaneous determination of L-DOPA and ACT, as evidenced by the well-separated voltammetric peaks ($\Delta E_p \approx 180$mV) in DPV measurements. The practical applicability of the Bi_2MoO_6/CPE was demonstrated by the successful determination of L-DOPA and ACT in real specimens.

Funding: *Not applicable.*

Conflicts of Interest: *The authors have no conflict of interest.*

References

[1] G. Gorle, A. Bathinapatla, S. Kanchi, Y. C. Ling, M. Rezakazemi, Low dimensional Bi_2Se_3 NPs/reduced graphene oxide nanocomposite for simultaneous detection of L-Dopa and acetaminophen in presence of ascorbic acid in biological samples and pharmaceuticals, J*ournal of Nanostructure in Chemistry* **12(4)** (2022) 513-528. https://doi.org/10.1007/s40097-021-00428-3

[2] M. Mazloum-Ardakani, S. H. Ahmadi, Z. S. Mahmoudabadi, A. Khoshroo, Nano composite system based on fullerene-functionalized carbon nanotubes for simultaneous determination of levodopa and acetaminophen, *Measurement* **91** (2016) 162-167. https://doi.org/10.1016/j.measurement.2016.05.035

[3] K. Movlaee, H. Beitollahi, M. R. Ganjali, P. Norouzi, Electrochemical platform for simultaneous determination of levodopa, acetaminophen and tyrosine using a graphene and ferrocene modified carbon paste electrode, *Microchimica Acta* **184** (2017) 3281-3289. https://doi.org/10.1007/s00604-017-2291-3

[4] K. Hatori, T. Kondo, Y. Mizuno, Levodopa absorption profile in Parkinson's disease: Evidence to indicate qualitative difference from the control, *Parkinsonism & Related Disorders* **2** (1996) 137-144. https://doi.org/10.1016/1353-8020(96)00011-9
[5] M. Mazloum-Ardakani, M. Zokaie, A. Khoshroo, Carbon nanotube electrochemical sensor based on and benzofuran derivative as a mediator for the determination of levodopa, acetaminophen, and tryptophan, *Ionics* **21** (2015) 1741-1749. https://doi.org/10.1007/s11581-014-1342-6
[6] T. Wang, N. N. Jafar, A. M. A. Al-Rihaymee, D. Y. Alhameedi, F. A. Rasen, F. S. Hashim, A. H. Alawadi, Highly efficient electrocatalytic oxidation of levodopa as a Parkinson therapeutic drug based on modified screen-printed electrode, *Heliyon* **10** (2024) e34689. https://doi.org/10.1016/j.heliyon.2024.e34689
[7] H. Yang, Z. Wei, S. He, T. Li, Y. Zhu, L. Duan, J. Wang, Fabrication of Electrochemical Sensor for Acetaminophen Based on Levodopa Polymer and Multi-walled Carbon Nanotubes Complex, *International Journal of Electrochemical Science* **12** (2017) 11089-11101. https://doi.org/10.20964/2017.12.50
[8] D. Dăscălescu, C. Apetrei, Voltammetric Determination of Levodopa Using Mesoporous Carbon-Modified Screen-Printed Carbon Sensors, *Sensors* **21** (2021) 6301. https://doi.org/10.3390/s21186301
[9] D. T. Hoang, F. Xing, D. Truong, Characteristics of pain symptoms in Parkinson's disease, *Clinical Parkinsonism & Related Disorders* **13** (2025) 100404. https://doi.org/10.1016/j.prdoa.2025.100404
[10] Z. Y. Li, D. Y. Gao, Z. Y. Wu, S. Zhao, Simultaneous electrochemical detection of levodapa, paracetamol and l-tyrosine based on multi-walled carbon nanotubes, *RSC Advances* **10** (2020) 14218-14224. https://doi.org/10.1039/D0RA00290A
[11] W. Si, W. Lei, Z. Han, Y. Zhang, Q. Hao, M. Xia, Electrochemical sensing of acetaminophen based on poly(3,4-ethylenedioxythiophene)/graphene oxide composites, *Sensors and Actuators B* **193** (2014) 823-829. https://doi.org/10.1016/j.snb.2013.12.052
[12] M. Sriramulu, J. S. Stephen Saviour, S. Balakrishnan, P. Kannaiyan, S. C. Gopinath, Advancements in Modified Electrodes with Electrochemical Sensors for Detecting Acetaminophen and Caffeine: An Update, *Critical Reviews in Analytical Chemistry* (2025) 1-27. https://doi.org/10.1080/10408347.2025.2496506
[13] A. Babaei, M. Sohrabi, Selective simultaneous determination of levodopa and acetaminophen in the presence of ascorbic acid using a novel TiO_2 hollow sphere/multi-walled carbon nanotube/poly-aspartic acid composite modified carbon paste electrode, *Analytical Methods* **8** (2016) 1135-1144. https://doi.org/10.1039/C5AY02497H
[14] T. T. Calam, Selective and Sensitive Determination of Paracetamol and Levodopa with Using Electropolymerized 3,5-Diamino-1,2,4-triazole Film on Glassy Carbon Electrode, *Electroanalysis* **33** (2021) 1049-1062. https://doi.org/10.1002/elan.202060477
[15] S. Zuliska, I. P. Maksum, Y. Einaga, G. T. M. Kadja, I. Irkham, Advances in electrochemical biosensors employing carbon-based electrodes for detection of biomarkers in diabetes mellitus, *ADMET and DMPK* **12** (2024) 487-527. https://doi.org/10.5599/admet.2361
[16] B. R. Adhikari, M. Govindhan, A. Chen, Carbon Nanomaterials Based Electrochemical Sensors/Biosensors for the Sensitive Detection of Pharmaceutical and Biological Compounds, *Sensors* **15** (2015) 22490-22508. https://doi.org/10.3390/s150922490
[17] W. Boumya, N. Taoufik, M. Achak, H. Bessbousse, A. Elhalil, N. Barka, Electrochemical sensors and biosensors for the determination of diclofenac in pharmaceutical, biological and water samples, *Talanta Open* **3** (2021) 100026. https://doi.org/10.1016/j.talo.2020.100026

[18] A. V. Bounegru, A. Dinu Iacob, C. Iticescu, P. L. Georgescu, Electrochemical Sensors and Biosensors for the Detection of Pharmaceutical Contaminants in Natural Waters-A Comprehensive Review, *Chemosensors* **13** (2025) 65. https://doi.org/10.3390/chemosensors13020065
[19] P. Manjunatha, Y. Arthoba Nayaka, H. T. Purushothama, R. O. Yathisha, M. M. Vinay, Single-walled carbon nanotubes-based electrochemical sensor for the electrochemical investigation of pantoprazole in pharmaceuticals and biological samples, *Ionics* **25** (2019) 2297-2309. https://doi.org/10.1007/s11581-018-2624-1
[20] M. Baghayeri, M. Namadchian, Fabrication of a nanostructured luteolin biosensor for simultaneous determination of levodopa in the presence of acetaminophen and tyramine: Application to the analysis of some real samples, *Electrochimica Acta* **108** (2013) 22-31. https://doi.org/10.1016/j.electacta.2013.06.069
[21] E. Fu, K. Khederlou, N. Lefevre, S. A. Ramsey, M. L. Johnston, L. Wentland, Progress on Electrochemical Sensing of Pharmaceutical Drugs in Complex Biofluids, *Chemosensors* **11** (2023) 467. https://doi.org/10.3390/chemosensors11080467
[22] C. Wang, J. Du, H. Wang, C. E. Zou, F. Jiang, P. Yang, Y. Du, A facile electrochemical sensor based on reduced graphene oxide and Au nanoplates modified glassy carbon electrode for simultaneous detection of ascorbic acid, dopamine and uric acid, *Sensors and Actuators B* **204** (2014)302-309. https://doi.org/10.1016/j.snb.2014.07.077
[23] F. Dong, L. Zhang, R. Li, Z. Qu, X. Zou, S. Jia, Electrochemical non-enzymatic biosensor for tyramine detection in food based on silver-substituted ZnO nano-flower modified glassy carbon electrode, *International Journal of Electrochemical Science* **16** (2021) 210234. https://doi.org/10.20964/2021.02.12
[24] H. Wang, A. Xie, S. Li, J. Wang, K. Chen, Z. Su, S. Luo, Three-dimensional g-C_3N_4/MWNTs/GO hybrid electrode as electrochemical sensor for simultaneous determination of ascorbic acid, dopamine and uric acid, *Analytica Chimica Acta* **1211** (2022) 339907. https://doi.org/10.1016/j.aca.2022.339907
[25] R. S. Mahale, V. K. Shamanth, K. Hemanth, R. Shashanka, P. C. Sharath, N. V. Sreekanth, lectrochemical Sensor Applications of Nanoparticle Modified Carbon Paste Electrodes to Detect Various Neurotransmitters, *Applied Mechanics and Materials* **908** (2022) 69-88. https://doi.org/10.4028/p-mizm85
[26] T. Thomas, R. J. Mascarenhas, P. Martis, Z. Mekhalif, B. K. Swamy, Multi-walled carbon nanotube modified carbon paste electrode as an electrochemical sensor for the determination of epinephrine in the presence of ascorbic acid and uric acid, *Materials Science and Engineering: C* **33** (2013) 3294-3302. https://doi.org/10.1016/j.msec.2013.04.010
[27] A. Ganash, S. Alshammari, E. Ganash, Development of a Novel Electrochemical Sensor Based on Gold Nanoparticle-Modified Carbon-Paste Electrode for the Detection of Congo Red Dye, *Molecules* **28** (2022) 19. https://doi.org/10.3390/molecules28010019
[28] J. G. Manjunatha, B. Kanthappa, N. Hareesha, C. Raril, A. M. Tighezza, M. D. Albaqami, Enhanced Electrochemical Detection of Rutin Using Poly (Methyl Orange) Modified Carbon Paste Electrode as a Responsive Electrochemical Sensor, *Chemistry Africa* ***7*** (2024) 1141-1150. https://doi.org/10.1007/s42250-023-00808-y
[29] B. D. Topal, C. E. Sener, B. Kaya, S. A. Ozkan, Nano-sized Metal and Metal Oxide Modified Electrodes for Pharmaceuticals Analysis, *Current Pharmaceutical Analysis* **17** (2021) 421-436. https://doi.org/10.2174/1573412916999200513110313
[30] M.R. Baezzat, Z. Pourghobadi, R. Pourghobadi, Nanomolar determination of Penicillin G potassium (PGK) salt using a Carbon Paste Electrode modified with TiO_2 nano particles /Ionic Liquids in real samples, *Materials Chemistry and Physics* **270** (2021) 124641. https://doi.org/10.1016/j.matchemphys.2021.124641

[31] M. Yang, P. H. Li, S. H. Chen, X. Y. Xiao, X. H. Tang, C. H. Lin, W. Q. Liu, Nanometal Oxides with Special Surface Physicochemical Properties to Promote Electrochemical Detection of Heavy Metal Ions, *Small* **16** (2020) 2001035. https://doi.org/10.1002/smll.202001035
[32] J. M. George, A. Antony, B. Mathew, Metal oxide nanoparticles in electrochemical sensing and biosensing, *Microchimica Acta* **185** (2018) 358. https://doi.org/10.1007/s00604-018-2894-3
[33] K. Jangid, R. P. Sahu, S. Sakib, I. Zhitomirsky, I. K. Puri, Surface-Modified Metal Oxides for Ultrasensitive Electrochemical Detection of Organophosphates, Heavy Metals, and Nutrients, *ACS Applied Nano Materials* **5** (2022) 17183-17193. https://doi.org/10.1021/acsanm.2c04105
[34] C. Zhu, Q. Wu, F. Yuan, J. Liu, D. Wang, Q. Zhang, Novel Electrochemical Sensor Based on MnO_2 Nanowire Modified Carbon Paper Electrode for Sensitive Determination of Tetrabromobisphenol A, *Chemosensors* **11** (2023) 482. https://doi.org/10.3390/chemosensors11090482
[35] N. H. Khand, I. M. Palabiyik, J. A. Buledi, S. Ameen, A. F. Memon, T. Ghumro, A. R. Solangi, Functional Co_3O_4 nanostructure-based electrochemical sensor for direct determination of ascorbic acid in pharmaceutical samples, *Journal of Nanostructure in Chemistry* **11** (2021) 455-468. https://doi.org/10.1007/s40097-020-00380-8
[36] Z. Amani-Beni, A. Nezamzadeh-Ejhieh, NiO nanoparticles modified carbon paste electrode as a novel sulfasalazine sensor, *Analytica Chimica Acta* **1031** (2018) 47-59. https://doi.org/10.1016/j.aca.2018.06.002
[37] N. P. Shetti, S. J. Malode, D. S. Nayak, G. B. Bagihalli, S. S. Kalanur, R. S. Malladi, K. R. Reddy, Fabrication of ZnO nanoparticles modified sensor for electrochemical oxidation of methdilazine, *Applied Surface Science* **496** (2019) 143656. https://doi.org/10.1016/j.apsusc.2019.143656
[38] M. Vazan, J. Tashkhourian, B. Haghighi, A novel electrochemical sensor based on MoO_3 nanobelt-graphene oxide composite for the simultaneous determination of paracetamol and 4-aminophenol, *Diamond and Related Materials* **140** (2023) 110549. https://doi.org/10.1016/j.diamond.2023.110549
[39] H. N. Ngoc, D. N. Xuan, P. V. Ngoc, T. Le Minh, T. P. Duc, T. Le Anh, $ZnCo_2O_4$ nanosheets as an efficient electrochemical sensing platform for determination of paracetamol, *Vietnam Journal of Science and Technology* **63** (2025) 347-363. https://doi.org/10.15625/2525-2518/19061
[40] B. S. Lou, U. Rajaji, S. M. Chen, T. W. Chen, A simple sonochemical assisted synthesis of $NiMoO_4$/chitosan nanocomposite for electrochemical sensing of amlodipine in pharmaceutical and serum samples, *Ultrasonics Sonochemistry* **64** (2020) 104827. https://doi.org/10.1016/j.ultsonch.2019.104827
[41] K. Venkatesh, R. Rajakumaran, S. M. Chen, C. Karuppiah, C. C. Yang, S. K. Ramaraj, B. M. A. Almunqedhi, A novel hybrid construction of $MnMoO_4$ nanorods anchored graphene nanosheets; an efficient electrocatalyst for the picomolar detection of ecological pollutant ornidazole in water and urine samples, *Chemosphere* **273** (2021) 129665. https://doi.org/10.1016/j.chemosphere.2021.129665
[42] J. Ganesamurthi, R. Shanmugam, S. M. Chen, K. Alagumalai, M.Balamurugan, C. H. Fan, A portable electrochemical sensor based on binary transition metal oxide (CoO/ZnO) for the evaluation of eugenol in real-time samples, *Surfaces and Interfaces* **38** (2023) 102845. https://doi.org/10.1016/j.surfin.2023.102845
[43] Y. Ma, Z. Wang, Y. Jia, L. Wang, M. Yang, Y. Qi, Y. Bi, Bi_2MoO_6 nanosheet array modified with ultrathin graphitic carbon nitride for high photoelectrochemical performance, *Carbon* **114** (2017) 591-600. https://doi.org/10.1016/j.carbon.2016.12.043
[44] Y. Ma, Y. Jia, L. Wang, M. Yang, Y. Bi, Y. Qi, Hierarchical nanosheet-based Bi_2MoO_6 nanotubes with remarkably improved electrochemical performance, *Journal of Power Sources* **331** (2016) 481-486. https://doi.org/10.1016/j.jpowsour.2016.09.084

[45] S. Bano, A. S. Ganie, R. I. A. Khan, S. Sultana, M. Z. Khan, S. Sabir, Designing and application of PPy/Bi_2MoO_6/chitosan nanocomposites for electrochemical detection of ciprofloxacin and benzene and evaluation of hydrogen evolution reaction, *Surfaces and Interfaces* **29** (2022) 101786. https://doi.org/10.1016/j.surfin.2022.101786

[46] J. A. Jesila, N. M. Umesh, S. F. Wang, G. Mani, A. A. Alothman, R. A. Alshgari, An electrochemical sensing of phenolic derivative 4-Cyanophenol in environmental water using a facile-constructed Aurivillius-structured Bi_2MoO_6, *Ecotoxicology and Environmental Safety* **208** (2021) 111701. https://doi.org/10.1016/j.ecoenv.2020.111701

[47] T. Ji, E. Ha, M. Wu, X. Hu, J. Wang, Y. Sun, J. Hu, Controllable Hydrothermal Synthesis and Photocatalytic Performance of Bi_2MoO_6 Nano/Microstructures, *Catalysts* **10** (2020) 1161. https://doi.org/10.3390/catal10101161